

Core Structure of Intracluster Gas: Effects of Radiative Cooling on Core Sizes

Takuya AKAHORI and Kuniaki MASAI

Department of physics, Tokyo Metropolitan University, Hachioji, Tokyo 192-0397
akataku@phys.metro-u.ac.jp, masai@phys.metro-u.ac.jp

(Received 2005 August 29; accepted 2006 April 8)

Abstract

We investigate the core structure of radiatively cooling intracluster gas, using a hydrodynamics code. We calculate evolution of model clusters of the initial core radii 160–300 kpc until the initial central cooling time, and analyze the resultant clusters using the double β -model as done by observational studies. It is found that the core-size distribution thus obtained shows two peaks ~ 30 –100 kpc and ~ 100 –300 kpc and marginally can reproduce the observed distribution which exhibits two distinct peaks around ~ 50 kpc and ~ 200 kpc. This result may suggest radiative-cooling origin for small cores, while cooling is yet insignificant in the clusters of large cores. It should be noted that the small core peak is reproduced by clusters that are still keeping quasi-hydrostatic balance before the initial central cooling time has elapsed.

Key words: galaxies: clusters: general — galaxies: evolution — X-rays: galaxies: clusters

1. Introduction

Profiles of X-ray emitting hot gas in clusters of galaxies have been studied often by using the so-called β -model, which is an isothermal hydrostatic gas model consisting of a core and envelope. From the β -model analyses of 121 clusters including nearby clusters (Mohr et al. 1999), Ota and Mitsuda (2002) obtained an interesting result that the distribution of the core radii of the intracluster gas exhibits two distinct peaks at ~ 50 kpc and ~ 200 kpc for $H_0 = 70 \text{ km s}^{-1} \text{ Mpc}^{-1}$ (see also Ota, Mitsuda 2004). Akahori and Masai (2005) (hereafter AM05) investigated correlations of the core radii with various properties of the clusters, and found that the radii in the larger core group around the peak ~ 200 kpc are marginally proportional to the virial radii of the clusters and therefore the origin may be attributed to simple self-similar collapse. On the other hand, in the smaller core group around ~ 50 kpc, no clear correlation is found between the core and virial radii, suggesting some other origin of the small core formation.

AM05 investigated several possibilities of the origin of the small cores, not only by examining correlations among the observational quantities but by simulating the β -model with a hydrodynamics code. Many of the small core clusters possess central cD's or giant ellipticals, but the simulation shows that the gas core under their presence is ~ 40 kpc at most, and is too small to account for the observed range ~ 40 –80 kpc. AM05 suggested another possibility: the effects of radiative cooling on the core size. Radiative cooling time is shorter in the core than in the ambient region, because the density is higher. As the core cools, the ambient gas then could inflow to compensate the pressure loss inside. Although the ASCA, Chandra and XMM-Newton observations (e.g., Makishima et al. 2001; Lewis et al. 2002; Peterson et al. 2001) suggested much smaller amount of cooled mass than expected for the clas-

sical cooling flow model (see Fabian 1994 for a review), this process increases the gas density toward the cluster center and is likely responsible for the small cores observed. AM05 found that the central cooling time, t_{cool} , is significantly shorter than the Hubble time for 48 out of 50 small core clusters.

Thermal evolution of clusters has been studied by many authors. Most of the papers addressed processes that would slow or inhibit the onset of radiative cooling instability, such as electron conduction and activities of active galactic nuclei. Until an elapsed time comparable to t_{cool} , however, the gas appears to be cooling rather slowly with the temperature $\sim \text{keV}$ at the cluster center. For example, Ruszkowski and Begelman (2002) studied the heating, conduction, and minimum temperature in cooling flows with a simple spherical model and showed that line and free-free cooling in the cluster center leads to slow cooling until the initial central cooling time has elapsed. At this stage feedback is not yet very important. Masai and Kitayama (2004) showed that when the intracluster gas is cooling with quasi-hydrostatic balancing, the temperature of the cooling gas appears to approach a constant value toward the cluster center.

In the present paper, we investigate thermal evolution of clusters, paying attention to the core radius of the intracluster gas undergoing radiative cooling. Our interest is the origin of the small cores or the observed core-size distribution which exhibits two distinct peaks. We simulate cooling clusters using a hydrodynamics code (AM05), and analyze the core radii applying the β -model, on which the observed results are based. In section 2 we describe the model. In section 3, we present the results of calculations and discuss the properties of the cooling cores. We give some concluding remarks in section 4.

2. Model and Calculations

We calculate the evolution of radiatively cooling intra-cluster gas which is initially in hydrostatic balance under the presence of dark matter. We analyze the resultant clusters using the β -model in the same manner as the observations (Ota, Mitsuda 2002): the core-radius distribution having two distinct peaks was obtained by analyses using the β -model. Since the β -model is based originally on the King model of the collisionless matter (see e.g., Sarazin 1986), we apply primarily the King model for the dark matter and galaxies of a cluster. We also mention the results in the case of the NFW dark matter model (Navarro et al. 1996), because such a cuspy profile has been suggested for dark halo mergers or cluster formation by numerical simulations. As for the thermal evolution of the intracluster gas, the two dark matter models show the similar results to each other. In the following we describe our models and calculations along the King dark matter model.

With the gravitational potential Φ of the total mass within radius r , gravitational balance of a spherically symmetric cluster is written as,

$$\begin{aligned} \Phi &= \frac{kT}{\mu m} \left(\frac{d \ln \rho_g}{d \ln r} + \frac{d \ln T}{d \ln r} \right) & : \text{gas} \\ &= \sigma_{*r}^2 \left(\frac{d \ln \rho_*}{d \ln r} + \frac{d \ln \sigma_{*r}^2}{d \ln r} \right) & : \text{dust} \end{aligned} \quad (1)$$

where ‘‘dust’’ means collisionless components, i.e. dark matter and galaxies, k is the Boltzmann constant, m the proton mass, μ the mean molecular weight for which we take $\mu = 0.6$, ρ the mass density for each component, T the gas temperature, and σ_r is the radial velocity dispersion which is equal to the line-of-sight velocity dispersion for the isotropic dust. If isothermal distribution is attained for every component, i.e. $d \ln T / d \ln r \simeq 0$ and $d \ln \sigma_{*r}^2 / d \ln r \simeq 0$,

$$\beta_{\text{prof}} \equiv \frac{d \ln \rho_g / d \ln r}{d \ln \rho_* / d \ln r} \simeq \frac{\sigma_{*r}^2}{kT / \mu m} \equiv \beta_{\text{spec}} \quad (2)$$

follows equation (1).

For comparison with the observations of core sizes, in modelling clusters we apply the density profile function based on the β -model (Cavaliere, Fusco-Femiano 1976),

$$\rho(r) = \rho_0 [1 + (r/r_c)^2]^{-3\beta/2}, \quad (3)$$

where ρ_0 is the central density, r_c is the core radius, and β is a parameter to represent the envelope slope. For the consistency with the β -model for the gas, we adopt the King model for the collisionless components. Although the original King model (King 1966) is not of simple analytic form, the profile may be approximated with equation (3), which is sometimes called approximate King model (see e.g., Sarazin 1986). Table 1 shows the best-fit parameters for the King profile with equation (3) in the range $r/r_K = 0.0$ – 10.0 , where r_K is the core radius of the King model.

Table 1. Best-fit parameters for the King profile.

Range	Fitting parameters		
	r_{c*}/r_K	$\rho_{0*}/\rho_K(0)$	β_*
0.0–1.0	1.04	1.00	1.13
0.0–2.0	1.05	1.00	1.14
0.0–5.0	1.10	1.00	1.21
0.0–10.0	1.34	0.98	1.46

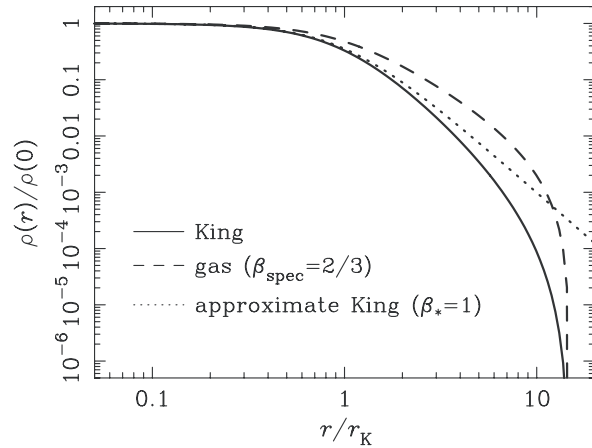


Fig. 1. Radial density profiles. The solid and dashed lines represent $\rho_* \propto \rho_K$ and $\rho_g \propto \rho_K^{2/3}$, respectively. The dotted line is the approximate King profile (equation (3) with $\beta = 1$).

We investigate four models of clusters which consist of dark matter, galaxies, and gas with their mass ratio $M_{\text{gal}} : M_{\text{gas}} : M_{\text{DM}} = 1 : 5 : 30$. The galaxies and dark matter are represented by their gravitational potential components in the momentum equation (equation (16) in AM05). We employ the original King model for their density distributions, and then $\rho_g \propto \rho_*^{\beta_{\text{spec}}}$ with $\beta_{\text{spec}} (\simeq \beta_{\text{prof}}) = 2/3$ for the initial gas profile (equation (2)). The initial profiles are shown in figure 1, where the tidal radius $r_t = r_{\text{vir}}$, i.e. $\rho_*(r \geq r_{\text{vir}}) = 0$, and the core radius $r_K = r_c$. The core radius of the gas well reflects the gravitational potential consistently in the context of the β -model (AM05).

The four model-clusters have different initial core radii of the gas, $r_c = 160, 200, 250,$ and 300 kpc, and satisfy the self-similar relation with their virial radii, as $x_{\text{vir}} \equiv r_{\text{vir}}/r_c = 15$, or $r_{\text{vir}} = 2.40, 3.00, 3.75,$ and 4.50 Mpc (listed in table 2). These values are on the dashed line in figure 5 of AM05, which represents the r_{vir}/r_c relation obtained for the large core group peaked at ~ 200 kpc in the observed core-size distribution. The initial gas temperature (isothermal), T , under the hydrostatic equilibrium is higher than the virial temperature, T_{vir} , as $\beta_{\text{spec}} T \simeq T_{\text{vir}}$ for $x_{\text{vir}}^2 / (1 + x_{\text{vir}}^2) \simeq 0.996$ (see AM05).

We carry out hydrodynamical simulations using a Smoothed Particle Hydrodynamics (SPH) code (Hernquist, Katz 1989; Monaghan 1992) with 95,000 bodies. The smoothing length is estimated to be $h = 17.1$ kpc

Table 2. Initial properties of the simulated clusters.

Model	r_{vir} (Mpc)	M_{vir}^* ($10^{15}M_{\odot}$)	T (keV)	β -model parameters**			
				r_c (kpc)	n_{g0} (0.01cm^{-3})	β	t_{cool}^{**} (Gyr)
(a).....	2.40	0.555	3.12	171	2.15	0.83	0.689
(b).....	3.00	1.08	4.87	209	2.16	0.82	0.800
(c).....	3.75	2.62	7.61	260	2.10	0.81	1.086
(d).....	4.50	3.66	11.0	310	2.04	0.80	1.303

* The virial mass.

** Values are estimated after 1.6 Gyr of the hydrostatic balance test without cooling.

and 9.97 kpc for the core region ($n_g \sim 0.02 \text{ cm}^{-3}$) and cooled cluster center ($n_g \sim 0.1 \text{ cm}^{-3}$), respectively, and sufficiently small compared with the core size concerned here. Here, $n_g = \rho_g/\mu m$ is the number density of the gas. For the general artificial viscosity we adopt the Monaghan-Gingold value (Monaghan, Gingold 1983; see also Hernquist, Katz 1989) with the coefficients (α , β) = (1.0, 2.0), and for the gravitational softening we take $\nabla\Phi \propto 1/(r^2 + \epsilon^2)$ with $\epsilon = 0.1h$.

Radiative cooling is taken into account for the energy equation as

$$\frac{du_i}{dt} = -\frac{P_i}{\rho_i^2} \nabla \cdot v_i - \rho_i \Lambda(T_i), \quad (4)$$

where u_i is the internal energy per unit mass, v_i is the velocity, and $\Lambda(T_i)$ is the cooling function for the i -th SPH-particle. No additional heating processes are considered because the evolution of cooling cores is of our interest. Neither is electron conduction, which is not effective within cooling cores. We use the cooling function of Sutherland and Dopita (1993), which includes line emission with the metallicity $Z \sim 0.3Z_{\odot}$, by approximation as $\Lambda(T_i) = 3.0 \times 10^{-27} T_i^{1/2} \text{ erg cm}^{-3} \text{ s}^{-1}$ in the temperature range $\sim 1.5\text{--}10 \text{ keV}$. Actually, until $t \sim t_{\text{cool}}$ of practical interest, the temperatures of the cooling gas are still above $\sim 1.5 \text{ keV}$ where bremsstrahlung dominates. Here, $t_{\text{cool}} = 3n_{g0}kT/(n_{g0}^2\Lambda)$ is the initial cooling time at the cluster center.

Before going to calculations of evolution with radiative cooling, we examine the hydrostatic balance of the gas with $\Lambda(T_i) = 0$ in equation (4), as shown in figure 2. Gravity on the gas and the pressure gradient balance with each other, and the initial gas profile is kept at least until 3.2 Gyr, which is enough long compared with the dynamical (free-fall) timescale, $t_d = (32/3\pi G\rho)^{1/2} \sim 1.6 \text{ Gyr}$ at the cluster center ($n_{g0} = 0.02 \text{ cm}^{-3}$). The gas is kept nearly isothermal so that the profile is well represented by the β -model, although the temperature declines somewhat at $r > 5r_c$ due likely to adiabatic expansion of the outermost envelope. At $r \leq 5r_c$ of practical interest, the hydrostatic gas is represented well by the β -model as follows. From equations (2) and (3), the β -model should give a relation

$$\beta_{\text{prof}} = \beta/\beta_* \simeq \beta_{\text{spec}}, \quad (5)$$

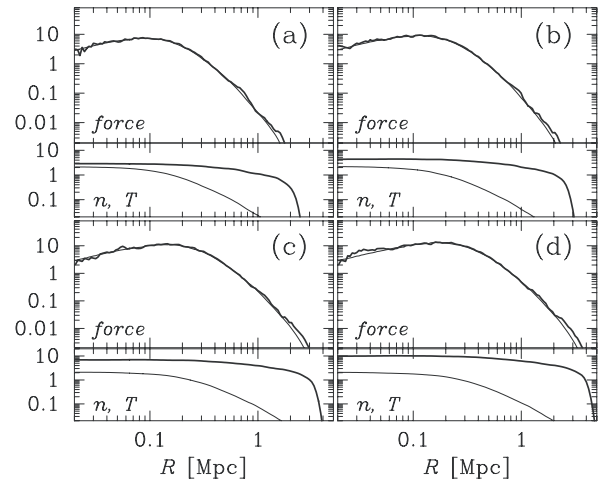


Fig. 2. Initial hydrostatic balance of the simulated clusters. We obtain the clusters after 1.6 Gyr of the hydrostatic balance test without cooling. For each box, the upper panel represents the gravity on the gas and the pressure gradient (the thin and thick line, respectively, in a unit $1.79 \times 10^{38} \text{ g cm s}^{-2}$), and the lower panel represents the density (the thin line, 0.01 cm^{-3}) and temperature (the thick line, keV).

or $\beta \simeq \beta_*\beta_{\text{spec}}$. Actually, $\beta \sim 0.80\text{--}0.83$ (table 2) is consistent with $\beta_*\beta_{\text{spec}} \sim 0.8$ for $\beta_* \sim 1.2$ (table 1) and $\beta_{\text{spec}} = 2/3$.

3. Results and Discussion

3.1. Evolutions of the β -Model Parameters

We apply the double β -model as well as the single β -model to simulated clusters. The double β -model is the superposition of two single β -models as

$$\rho(r) = \rho_1[1 + (r/r_1)^2]^{-3\beta_1/2} + \rho_2[1 + (r/r_2)^2]^{-3\beta_2/2}. \quad (6)$$

While in observations the parameters are inferred from the surface brightness profile, which depends substantially on the density profile as $\propto \rho^2 T^{1/2}$, in our calculations they are obtained straightforwardly from the density profile. We obtain the best-fit parameters of the “outer” components (ρ_1 , r_1 , and β_1) using the data in the range $1.0 \leq r/r_K \leq 5.0$, and then obtain the “inner” ones (ρ_2 and r_2), assuming $\beta_2 = \beta_1$ as done by Ota and Mitsuda

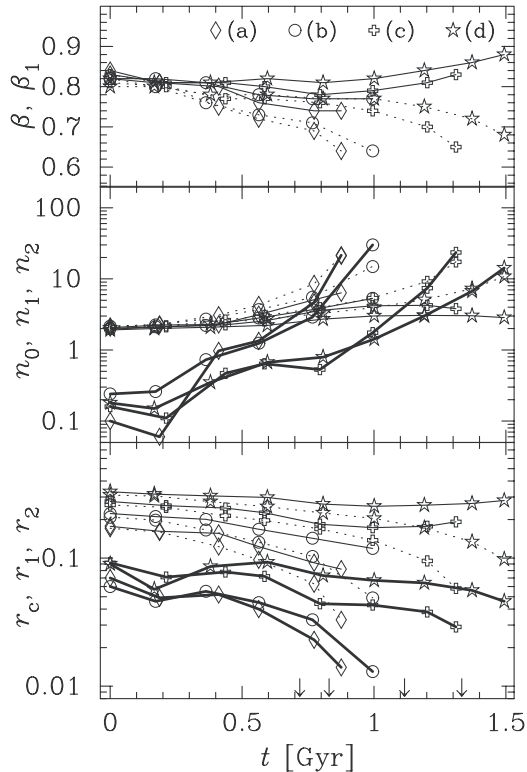


Fig. 3. Thermal evolutions of the β -model parameters: slope parameter (the top panel), number density of center (the middle, in a unit 0.01 cm^{-3}), and core radius (the bottom, Mpc). The thin and thick solid lines represent the outer and inner components of the double β -model, respectively. The dotted lines represent the components of the single β -model. The arrows represent the cooling time of each cluster.

(2002; 2004), using the data of $0.0 \leq r/r_K \leq 5.0$ including the outer component with ρ_1 , r_1 and β_1 fixed.

Figure 3 shows the time evolution of the parameters for the single and double β -models after the gas starts to cool. We see in the bottom panel that the outer core radii (the thin solid lines) decrease very slowly compared with the core radii of the single β -model (the dotted lines). This implies that the outer component keeps the initial value since thermal evolution of the gas is predominant in the inner component. Actually, β_1 , which is determined by the outer component, is roughly kept the initial value, although β of the single β -model decreases by about 10% within t_{cool} (the top panel). The behavior is also seen in the central density. While the increase in the central density of the outer component is as small as a factor of ~ 2 , the central density with the single β -model increases exponentially (the middle panel).

From the time evolution of the core radii, we calculate the time during which a cluster would have the core radius between r and $r + \Delta r$ and estimate the population or relative number of clusters that would fall into a certain range of core radius. The core size distribution thus obtained for the outer and inner cores is shown in figure 4. Our calculations reproduce the observed core-size distribution or two distinct peaks except for the details such

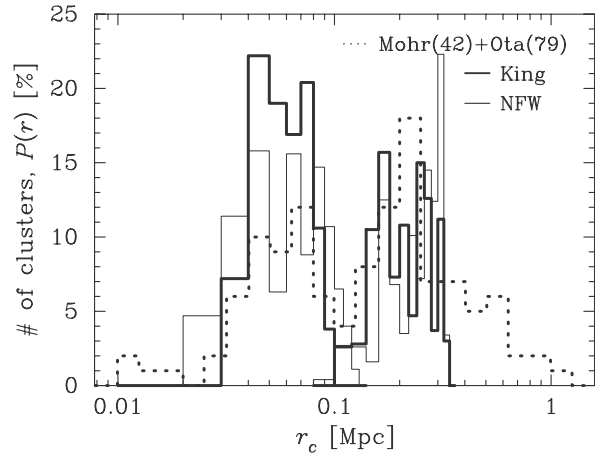


Fig. 4. Distribution of core radii. The thick solid lines represent the relative probabilities within t_{cool} of the four simulated clusters, estimated for the outer and inner cores with the bin of $\Delta r = 20 \text{ kpc}$ and 10 kpc , respectively. The dotted line represents the distribution of core radii of 121 clusters (same as figure 4 of AM05). The thin solid lines represent the relative probabilities for the case of the NFW dark matter potential.

as their widths or the tails. This implies that radiative cooling is a possible cause of small cores of clusters, while cooling is yet minor in large core clusters. It is interesting that even the small core peak is produced by the clusters of $t \lesssim t_{\text{cool}}$, i.e. moderately cooled clusters that are keeping quasi-hydrostatic balance.

In the observed distribution of figure 4 one may notice four clusters which have very small cores. It is unlikely that such small cores as $r_c \lesssim 30 \text{ kpc}$ are reproduced by radiative cooling within $t \lesssim t_{\text{cool}}$. Our cooling function underestimates by $\sim 40 \%$ at $T = 1.5 \text{ keV}$ compared with the function of Sutherland and Dopita (1993). If applied their original function, the small core peak might have a tail toward the small core end. However, this is unlikely because such a very small core is quite transient (figure 3). This may be related with the fact that clusters of $t \gtrsim t_{\text{cool}}$ are out of quasi-hydrostatic balance. Another possible explanation of the very small cores is the presence of central gravitational source; the four clusters evidently have central cD's or giant ellipticals. The presence of such galaxies is likely responsible for the very small cores (see AM05).

The lack of clusters of core radii $\sim 120 \text{ kpc}$ is seen in the calculated distribution as well. Although the outer cores of $\sim 100\text{--}300 \text{ kpc}$ of simulated clusters can explain the population around the peak of the observed large core clusters, the latter exhibits larger core tail extended to $r_c \sim 1 \text{ Mpc}$. If we simulate clusters which have initial huge cores $\gtrsim 0.4 \text{ Mpc}$, we might get the cooled cores of $\sim 120 \text{ kpc}$ following the self-similarity (see below). However, if such huge core clusters are in hydrostatic equilibria as represented by the β -model, the clusters would have unlikely virial radii as large as $r_{\text{vir}} \gtrsim 6 \text{ Mpc}$. In fact, most of the huge core clusters deviate from the self-similar relation, as shown in figure 5 of AM05.

A considerable factor for the origin of such huge cores is mergers. When merger takes place, the gas could form a large flat core with a steep envelope (large β). Actually, in AM05 sample, 6 out of 7 clusters of $\beta > 1$ have cores of $r_c > 0.6$ Mpc, and the average of β in the 17 clusters (including 14 irregulars) of $r_c > 0.4$ Mpc is 0.98, which is significantly greater than the average 0.65 in 121 clusters.

We find in figure 3 that the single β -model represents the intermediate profile between the inner and outer profiles of the double β -model. If cooling is minor and the self-similarity remains, the profile would be represented by the single β -model of a large core. With cooling the core, but yet minor in the outer, the profile is being that represented better but transiently by the double β -model, and eventually comes to that represented by the single β -model of a small core. As a result, the core-size distribution exhibits two distinct peaks along the thermal evolution. Two distinct peaks are not seen for the cluster sample of redshift between 0.4 and 1.3 (Ettori et al. 2004). The reason may be that their analysis was done with the single β -model; otherwise, the cooling might be yet minor in such very distant clusters. We confirm that two distinct peaks do not appear if applied the single β -model to the simulated clusters. The estimation of the inner core radius depends on β_1 obtained from the outer slope. If β_1 is taken to be 10 % smaller than that in the present calculations, the resultant clusters might have 10 % smaller cooling cores, as expected from the β - r_c correlation described in figure 1. Thus, the small-core distribution merely shifts toward the smaller side.

We also investigate clusters of the NFW dust profile (Navarro et al. 1996), where the parameters of the NFW profile are determined so that the clusters have nearly the same initial density and temperature profiles of the gas, and analyze the core sizes in the same manner as above. The obtained core-radius distribution is similar except for a few % tail extended to ~ 20 kpc (figure 4). There is no appreciable difference between the NFW and King dark matter models in the cooling gas distribution.

The evolutions of the density and temperature profiles (figure 5) imply the self-similar evolution in the core region, since the evolution is predominant in the inner component. We try to approximate the evolution of inner-core radii with a parameter, ϵ , and the normalized time, $\tau \equiv t/t_{\text{cool}}$, as

$$r_2 = r_{2,0}(1 - \epsilon\tau). \quad (7)$$

Figure 6 shows that equation (7) can represent the inner-core evolution, i.e. thermal evolution of the small core can be described by the self-similar relation, normalized by t_{cool} and $r_{2,0}$ which are obtained from the initial outer component. This self-similarity may be seen also in the clusters having different initial central densities, because in the β -model the central density determines the amplitude of the profile while the flat-core region clearly exists; the core radius is related mainly to the envelope slope (see figure 1).

Such a self-similarity is, however, likely lost in the observed small cores. At the initial state, the inner-core size

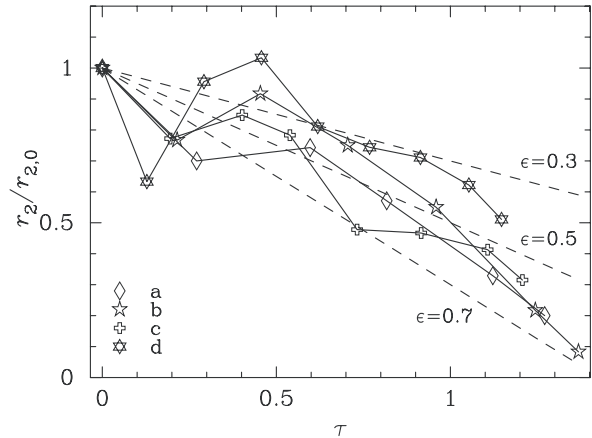


Fig. 6. Thermal evolutions of inner-core radii. The dashed lines represent equation (7) with $\epsilon = 0.3, 0.5, 0.7$.

can be represented by the outer-core size, as

$$r_{2,0} = \alpha r_{1,0}, \quad (8)$$

where $\alpha \sim 0.3$ is obtained from figure 3. While the thermal evolution is predominant in the inner component, outer core is roughly constant, i.e. $r_1 \simeq r_{1,0}$, so that $\delta r_2 \equiv r_{2,0} - r_2$ is written with equations (7) and (8) as

$$\delta r_2 \simeq \alpha \epsilon \frac{r_{1,0}}{t_{\text{cool}}} t. \quad (9)$$

From equations (10) and (11) in AM05, the initial central cooling time is given by

$$t_{\text{cool}} \propto \left(\beta \frac{x_{\text{vir}}^2}{1 + x_{\text{vir}}^2} \right)^{-1/2} r_{1,0}. \quad (10)$$

Therefore, equation (9) is written as

$$\delta r_2 \propto \alpha \epsilon \beta^{-1/2} t \quad (11)$$

for the clusters with $x_{\text{vir}} \gg 1$ (AM05). Equation (11) suggests that the self-similar relation in the small cores may be lost for not only the different age of the cluster from the last major merger, i.e. the time when the cluster formed to the current size and down to the hydrostatic equilibrium, which is labeled by t , but the various values of β from ~ 0.6 to ~ 1.0 in observed clusters as mentioned in AM05.

3.2. Evolution of Hydrostatic Structure

Calculations show that the cooling gas approximately keeps the hydrostatic balance between the gravitational force and pressure gradient at each step until $\sim t_{\text{cool}}$ (figure 7). We compare our result with quasi-hydrostatic cooling discussed by Masai and Kitayama (2004). They suggest that $\dot{M}_r \sim \tilde{M}_r / \tilde{t}_{\text{cool}}$ at every r or

$$C(r) \equiv (\tilde{M}_r / \tilde{t}_{\text{cool}}) / \dot{M}_r \sim \text{constant}, \quad (12)$$

where $\dot{M}_r = 4\pi\rho_g r^2 dr/dt$ is the continuity equation, $\tilde{M}_r = 4\pi r^3 \rho_g / 3$ and $\tilde{t}_{\text{cool}} = 3n_g kT / (n_g^2 \Lambda)$ are the mass of a uniform gas sphere and the cooling time for the local values

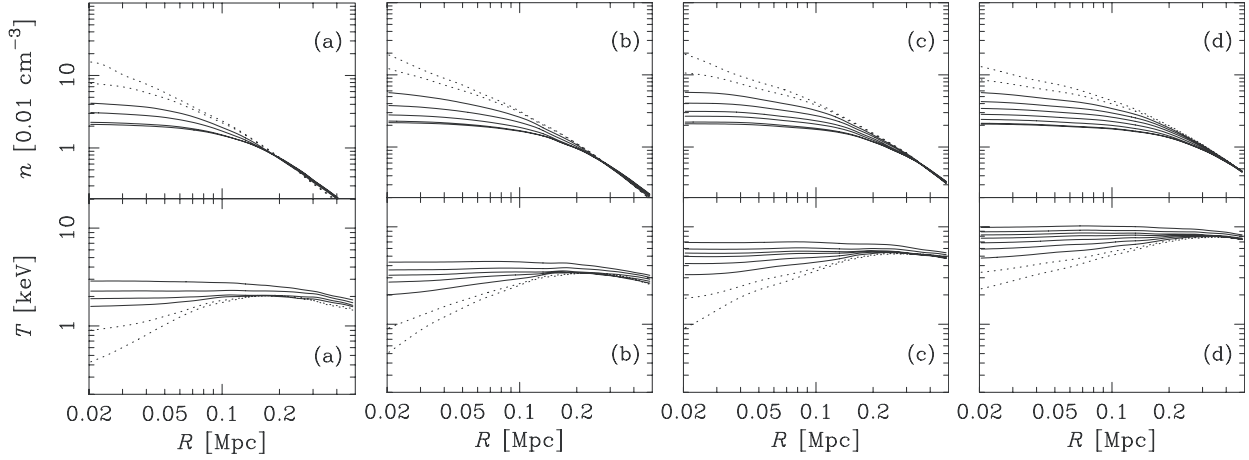


Fig. 5. Thermal evolutions of the density and temperature profiles of the four simulated clusters. The lines are drawn for intervals of about ~ 200 Myr until t_{cool} . Dotted lines represent the profiles for continuing calculations over t_{cool} , which are excluded for the analysis in figure 4.

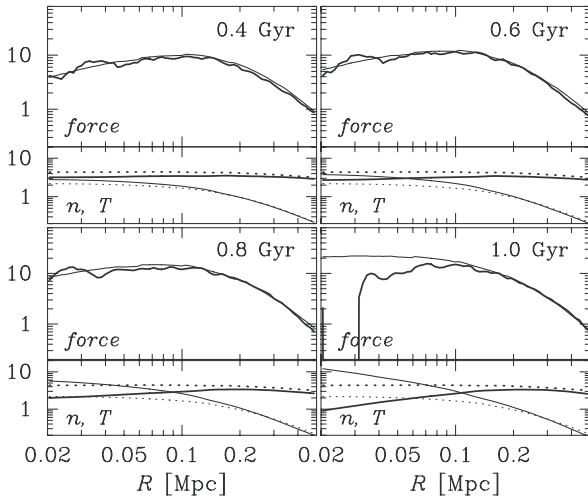


Fig. 7. Hydrostatic balance of cluster (b) after 0.4 ($0.5 t_{\text{cool}}$), 0.6 ($0.75 t_{\text{cool}}$), 0.8 (t_{cool}), and 1.0 ($1.25 t_{\text{cool}}$) Gyr. The lines are the same descriptions as figure 2. The dotted lines are the initial values of the density and temperature.

at radius r , respectively. As shown in figure 8, our calculation shows $C(r)$ is nearly constant. Until $\sim t_{\text{cool}}$, constant C is seen commonly for all the model clusters, not only the King case but also the NFW case.

Masai and Kitayama (2004) show some properties of quasi-hydrostatic cooling by approximating the density/temperature profiles in the power-law form. We examine our results in the same manner with $\rho_g \propto r^\alpha$, $T \propto r^\eta$ and inflow velocity $v_{\text{in}} \propto r^\zeta$. Since $C(r) \propto r^{1+\alpha-\eta/2-\zeta}$, quasi-hydrostatic cooling means $1 + \alpha - \eta/2 - \zeta \sim 0$ or

$$\alpha \sim -1 + \eta/2 + \zeta. \quad (13)$$

Such a relation is actually found at ~ 40 kpc: $\alpha = -0.42$ is comparable to $-1 + \eta/2 + \zeta \sim -0.41$ with $(\eta, \zeta) = (0.28, 0.45)$. At ~ 70 kpc, however, $\alpha = -0.63$ is smaller than $-1 + \eta/2 + \zeta \sim -0.54$ with $(\eta, \zeta) = (0.25, 0.34)$. Therefore,

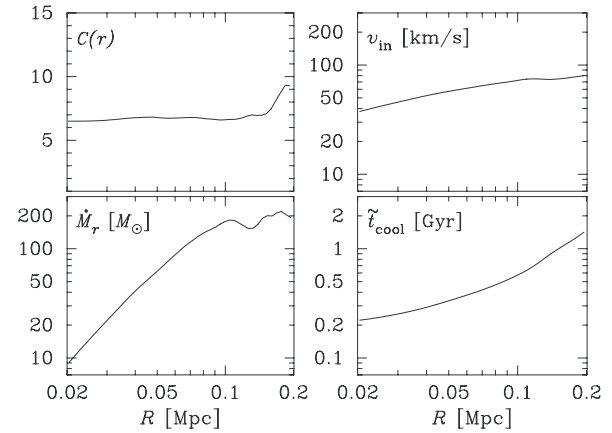


Fig. 8. $C(r) (\equiv (\tilde{M}_r/\tilde{t}_{\text{cool}})/\dot{M}_r)$, the inflow velocity (v_{in}), the mass flow rate (\dot{M}_r), and the cooling time (\tilde{t}_{cool}) after 0.8 Gyr (t_{cool}) of cluster (b).

quasi-hydrostatic balance may be satisfied marginally. When the cluster center cools rapidly at $t > t_{\text{cool}}$ (figure 5), the balance breaks because a large amount of inflow is required to maintain the balance. This also leads to the fact that the spatial resolution in calculations becomes practically worse than estimated simply from the number of SPH particles.

At $r \lesssim 100$ kpc, the gas inflow velocity $v_{\text{in}} \sim 0.1c_s$, where c_s is the sound speed. The mass inflow rate $\dot{M}_r(100 \text{ kpc}) \sim 200 M_\odot$ is decreasing to $\dot{M}_r(20 \text{ kpc}) \sim 10 M_\odot$, which are much smaller than expected for the classical cooling flow model and consistent with the quasi-hydrostatic cooling model by Masai and Kitayama (2004). It should be noted that they consider $\zeta < 0$ for smooth inflow, but we find in figure 8 that the inflow velocity gradually decreases toward the cluster center, i.e. $\zeta > 0$ rather than $\zeta < 0$. It is, however, consistent with their prediction that $\tilde{t}_{\text{cool}} \propto r^{1-\zeta}$ is well satisfied in $r < 100$ kpc.

$\zeta > 0$ implies that the gas is heated by viscosity.

We confirmed the convergence of the solution by using SPH-particles greater than $\sim 30,000$, which is also sufficient resolution to remove improperly accelerating cooling (Springel, Hernquist 2002). The gas inflow might be exaggerated by underestimating the viscous heating at the dead center of the cluster, though the influence reaches up likely to $\sim 2h$ from the center because SPH-particles within $2h$ at a given point contribute to the smoothed estimate in the present work. Therefore, at each step until $\sim t_{\text{cool}}$, quasi-hydrostatic balance is likely attained without some heat sources such as electron conduction and/or AGN activities.

4. Concluding Remarks

We investigate the thermal evolution of cluster cores: the core size of the intracluster gas can vary as the gas cools radiatively and flows toward the cluster center. In order to compare with the observed core radii, we apply the β -model or double β -model, as done by the observational studies, to analyze the gas profile, although the model is not always good for cooling cores of more or less center-peaked profiles. Thermal evolution of the gas may be classified into the following three stages: (I) at $\tau \equiv t/t_{\text{cool}} \lesssim 0.5$, the profile is represented by the single β -model with a large core or by the outer-core dominated double β -model, (II) at $0.5 \lesssim \tau \lesssim 1$, the profile is represented well by the double β -model, and (III) at $\tau \gtrsim 1$, the profile is represented by the single- β model with a small core or by the inner-core dominated double β -model.

Until $\sim t_{\text{cool}}$, which is the central cooling time for the initial gas profile, the gas cools keeping the hydrostatic balance between the gravity on the gas and the gradient of the thermal pressure. This evolution is explained by the quasi-hydrostatic cooling model proposed by Masai and Kitayama (2004). The properties of the cooling gas in our calculations, such as the mass inflow rate, radius dependence of the local cooling time and constant C , are consistent with this model in the regime where quasi-hydrostatic structure is attained. We find that the inflow velocity of the gas decreases toward the cluster center, and its mass flow rate is about $10 M_{\odot}$ at 20 kpc. Quasi-hydrostatic condition is marginally satisfied up to $t \sim t_{\text{cool}}$, and then the cluster center cools rapidly. Regarding the relation with the core-size distribution, it may be an important clue for understanding thermal properties of clusters that even the small core peak is produced by clusters of $t \lesssim t_{\text{cool}}$, in other words, by clusters that are still keeping quasi-hydrostatic balance.

Analyzing the simulated clusters with the single and double β -models, we demonstrate the core size distribution exhibits two distinct peaks at ~ 100 – 300 kpc and at ~ 30 – 100 kpc with a valley at ~ 120 kpc until t_{cool} and is in fairly good agreement with the observed distribution (Ota and Mitsuda 2002; Akahori and Masai 2005). This implies that the origin of small cores can be explained by radiative cooling or thermal evolution of the gas. However, a question remains: the self-similarity is kept in simulated clusters through the thermal evolution with cooling, but

seems to be lost in the observed small core clusters for the various values of β from ~ 0.6 to ~ 1.0 (Akahori and Masai 2005).

The authors would like to thank Tetsu Kitayama for his help for computation resources, and him and Naomi Ota for their useful discussions.

References

- Akahori, T., & Masai, K. 2005, PASJ, 57, 419
 Cavaliere, A., & Fusco-Femiano, R. 1976, A&A, 49, 137
 Ettori, S., Tozzi, P., Borgani, S., & Rosati, P. 2004, A&A, 417, 13
 Fabian, A. C. 1994, ARA&A, 32, 277
 Hernquist, L., & Katz, N. 1989, ApJS, 70, 419
 King, I. R. 1966, AJ, 71, 64
 Lewis, A. D., Stocke, J. T., & Buote, D. A. 2002, ApJ, 573, L13
 Makishima, K., et al. 2001, PASJ, 53, 401
 Masai, K., & Kitayama, T. 2004, A&A, 421, 815
 Mohr, J. J., Mathiesen, B., & Evrard, A. E. 1999, ApJ, 517, 627
 Monaghan, J. J. 1992, ARA&A, 30, 543
 Monaghan, J. J., & Gingold, R. A. 1983, J. Comput. Phys., 52, 374
 Navarro, J. F., Frenk, C. S., & White, S. D. M., 1996 ApJ, 462, 563
 Ota, N., & Mitsuda, K. 2002, ApJ, 567, L23
 Ota, N., & Mitsuda, K. 2004, A&A, 428, 757
 Peterson, J. R., et al. 2001, A&A, 365, L104
 Ruszkowski, M., & Begelman, M. C. 2002, ApJ, 581, 223
 Sarazin, C. L. 1986, Rev. Mod. Phys. 58, 1
 Springel, V., & Hernquist, L. 2002, MNRAS, 333, 649
 Sutherland, R. S., & Dopita, M. A. 1993, ApJS, 88, 253